# Solution conformation of several free tRNA$^{Leu}$ species from bean, yeast and *Escherichia coli* and interaction of these tRNAs with bean cytoplasmic Leucyl-tRNA synthetase. A phosphate alkylation study with ethylnitrosourea

André Dietrich[+], Pascale Romby, Laurence Maréchal-Drouard[+], Pierre Guillemaut[§] and Richard Giegé*

Laboratoire de Biochimie, Institut de Biologie Moléculaire et Cellulaire du CNRS, 15, rue René Descartes, F-67084 Strasbourg Cedex, France

Received March 9, 1990; Accepted April 9, 1990

## ABSTRACT

**The solution conformation of eight leucine tRNAs from *Phaseolus vulgaris*, baker's yeast and *Escherichia coli*, characterized by long variable regions, and the interaction of four of them with bean cytoplasmic leucyl-tRNA synthetase were studied by phosphate mapping with ethylnitrosourea. Phosphate reactivities in the variable regions agree with the existence of RNA helices closed by miniloops. At the junction of these regions with the T-stem, phosphate 48 is strongly protected, in contrast to small variable region tRNAs where P49 is protected. The constant protection of P22 is another characteristics of leucine tRNAs. Conformational differences between leucine isoacceptors concern the anticodon region, the D-arm and the variable region. In several parts of free tRNA$^{Leu}$ species, e.g. in the T-loop, phosphate reactivities are similar to those found in tRNAs of other specificities, indicating conformational similarities among tRNAs. Phosphate alkylation of four leucine tRNAs complexed to leucyl-tRNA synthetase indicates that the 3'-side of the anticodon stem, the D-stem and the hinge region between the anticodon and D-stems are in contact with the plant enzyme.**

## INTRODUCTION

Transfer ribonucleic acids specific for leucine are of particular interest. From a structural point of view these tRNAs, like those specific for serine and, in prokaryotes, for tyrosine, are characterized by a large variable region or extra-loop (1). Although several tRNA$^{Leu}$ species have been crystallized (2–5), no X-ray study could be undertaken up to now, mainly due to the poor diffracting quality of the crystals. As a consequence, no three-dimensional structural informations, except modelling data (6, 7), are available and in particular the exact conformation of the variable loop in these tRNAs is unknown. Also, apart from indirect data originating from sequence comparisons (8, 9), no direct biochemical informations as to the interaction sites of tRNA$^{Leu}$ with leucyl-tRNA synthetase are yet available. From another point of view tRNA$^{Leu}$ isoacceptors exhibit a great variability in sequences and an important structural heterogeneity in the anticodon region due to the degeneracy of leucine codons (1, 10). This raises the problem of the relationship between structure and function, in particular at the level of the anticodon region which has been proposed as a recognition site for aminoacyl-tRNA synthetases in several systems (11).

The present work is a comparative study of the solution conformation of several isoaccepting species of tRNA$^{Leu}$ originating from the higher plant *Phaseolus vulgaris*, the yeast *Saccharomyces cerevisiae* and the bacterium *Escherichia coli*. Ethylnitrosourea was the structural tool employed. It is a reagent alkylating preferentially oxygen atoms of phosphate groups. Its use for structural studies in the RNA field was validated on yeast tRNA$^{Asp}$ and tRNA$^{Phe}$, molecules for which a three-dimensional structure was available. It was shown that most, if not all, chemical data can be accounted by the crystallographic structure of these two tRNAs (12). As a consequence, the probe was used on other tRNAs (e.g. 13, 14) and structural rules could be defined allowing to predict conformations in tRNAs for which no crystallographic data are available (15). The present work brings experimental evidence that structural features common to all class I tRNAs mapped so far with ethylnitrosourea are also found in leucine-specific tRNAs. This is for instance the case for the T-loop conformation. In addition, ethylnitrosourea mapping revealed specific features which likely are characteristics of large variable region tRNAs. Also differences between the isoacceptors were revealed, in particular within the variable region.

Ethylnitrosourea was also found as a powerfull tool to footprint

* To whom correspondence should be addressed

Present addresses: [+]Institut de Biologie Moléculaire des Plantes du CNRS and Université Louis Pasteur, 12 rue du Gal. Zimmer, F-67000 Strasbourg and [§]Institut Universitaire de Technologie Louis Pasteur, 3 rue de l'Argonne, F-67000 Strasbourg, France

contact points of tRNAs with aminoacyl-tRNA synthetases. The relevance of the method was already discussed for several tRNA/aminoacyl-tRNA synthetase systems (e.g. 13, 14, 16, 17) and, in particular, it was shown that low resolution X-ray data on the $tRNA^{Asp}$/aspartyl-tRNA synthetase complex (18) fit the ethylation protection data on this system (12). Experiments on four leucine specific tRNAs complexed with bean leucyl-tRNA synthetase are presented here. They show alkylation protections by this synthetase of several homologous phosphates, some of them located in the anticodon stem. These results represent the first structural investigation at the three-dimensional level on plant tRNAs free or complexed with an aminoacyl-tRNA synthetase. They will be compared with those found in other tRNA/synthetase systems.

## MATERIALS AND METHODS

### $tRNA^{Leu}$ species and plant leucyl-tRNA synthetase

Bean *(Phaseolus vulgaris)* chloroplastic $tRNA^{Leu}$(U*AA), $tRNA^{Leu}$(CmAA) and $tRNA^{Leu}$($UAm^7G$) and cytoplasmic $tRNA^{Leu}$(C*AA) were purified from bean leaves as previously described (19, 20). Yeast cytoplasmic $tRNA^{Leu}$(UAG) and $tRNA^{Leu}$($m^5CAA$), *E. coli* $tRNA^{Leu}$(CAG) and $tRNA^{Leu}$(GAG) were prepared by established procedures starting with counter-current distribution followed by chromatographies on Sepharose 4B and RPC 5 (21, 22). Nucleotide sequences of these tRNAs are found in the compilation by Sprinzl *et al.* (1). To note is the existence of a C2-G71 base-pair in chloroplastic $tRNA^{Leu}$(CmAA) (23), instead of the G2-U71 base pair previously described (19, 24).

Bean cytoplasmic leucyl-tRNA synthetase is a monomeric synthetase of $M_r$ 130,000. It was purified as described (22) and stored at −20°C as a concentrated stock solution at 2.0 $mg.ml^{-1}$ in 50 mM potassium phosphate buffer pH 7.5 containing 50% (v/v) glycerol, 10% (v/v) propanediol, 1 mM $MgCl_2$, 0.1 mM EDTA, and 5 mM β-mercaptoethanol.

### Alkylation of tRNAs by ethylnitrosourea

Experiments were done on 3′ end-labeled tRNAs after restoring the CCA-end with [α-$^{32}$P]ATP (Amersham, 400 Ci/mmol) and yeast tRNA nucleotidyltransferase (25) on molecules previously treated with snake venom phosphodiesterase (VDP grade, Worthington, Freehold, USA). Labeled tRNAs were purified by electrophoresis on 15% polyacrylamide/8M urea slab gels. Before alkylation reactions, tRNAs were renatured by heating at 50°C for 5 min and slowly cooling to room temperature after addition of 10 mM $MgCl_2$. Experimental details are described elsewhere (26).

Control experiments with unlabeled tRNAs subjected to the treatments done prior to alkylation were run in order to check whether these treatments lead to an irreversible inactivation of the molecules. It was found that all tRNAs, including yeast cytoplasmic $tRNA^{Leu}$($m^5CAA$) which can exist under certain circumstances in a metastable and inactive form (27, 28), recover their full aminoacylation activity after the final renaturing step, thus demonstrating that tRNAs used for ethylation experiments are in their native conformation.

Statistical alkylation of phosphate residues in $tRNA^{Leu}$ species, either free or complexed with leucyl-tRNA synthetase, was conducted following essentially methodologies described elsewhere (16, 26). Alkylations were done at 20°C for 2 h in 150 mM sodium cacodylate buffer (pH 8.0) containing 10 mM $MgCl_2$. Ethylnitrosourea was added as a saturated ethanolic solution (5 μl) to 20 μl aqueous buffer containing either tRNA alone or both tRNA and leucyl-tRNA synthetase. The final concentration of the reagent in the incubation mixtures was 140 mM and that of labeled and non-radioactive carrier tRNA was 1 μM. Leucyl-tRNA synthetase was 3 μM. Alkylation on free tRNA under denaturing conditions was conducted at 80°C for 2 min in 150 mM sodium cacodylate buffer (pH 8.0) containing 1 mM EDTA. Control experiments, in which ethanol was substituted for the ethanolic ethylnitrosourea solution, were undertaken on free or complexed tRNA in order to distinguish between cuts generated by alkylation or degradations. After the alkylation reactions, the tRNAs were split at the phosphotriester positions in Tris-HCl buffer (pH 9.0) as described (26). The liberated oligonucleotides were then analyzed by electrophoresis on denaturing polyacrylamide gels. The assignment of the bands was done by comparison with partial ribonuclease T1 digests. Due to methodological difficulties phosphates at the 5′ and 3′-termini of tRNAs could not be assigned. Phosphate alkylation patterns were quantitatively evaluated by densitometric measurements of autoradiograms.

For footprinting of tRNAs complexed with leucyl-tRNA synthetase, it was verified that the alkylation conditions at pH 8.0 guarantee complex formation and that the four leucine-specific tRNAs (see Table I) tested for their interactions with bean cytoplasmic leucyl-tRNA synthetase are fully chargeable by this bean enzyme. Reactions were performed under rather high ionic strength and in the presence of $MgCl_2$ in order to favor the specific interactions. It was also verified that ethylnitrosourea does not inhibit the aminoacylation reaction catalyzed by bean cytoplasmic leucyl-tRNA synthetase and that the different leucine tRNAs can be efficiently charged by this enzyme under the conditions used for alkylation, showing that the specific complex is formed.

All experiments were at least triplicated, and several tRNA species were always run in parallel on the same gel. In particular, for footprinting experiments, the four different $tRNA^{Leu}$/leucyl-tRNA synthetase complexes were tested together in the same comparative experiment. Quantitative measurements of individual experiments were averaged to yield the phosphate reactivity patterns presented in Figs. 2 and 3. Accuracy was estimated as ±15%.

## RESULTS AND DISCUSSION

### Solution mapping of several native $tRNA^{Leu}$ species

Phosphate mapping experiments were conducted on two families of leucine tRNAs, the first one of prokaryotic type comprising three bean chloroplastic species and two *E. coli* tRNAs, and the second one including three eukaryotic tRNAs, one from bean and two from yeast. All these tRNAs are of class II and their general structural features are listed in Table I. To note here are the sequence differences between prokaryotic and eukaryotic species, in particular for the differential location of the two constant guanines G18 and G19, which should consequently lead to different D-T loop orientations.

Alkylation of phosphates by ethylnitrosourea leads to chain breakage of the ribose-phosphate backbone of tRNA which can be revealed on sequencing gels. When conducted under conditions where the conformation of the tRNA is maintained, only those phosphates accessible in the three-dimensional structure of the RNA will react. Their positions in the sequence of the tRNA

**Table I.** Structural features in $tRNA^{Leu}$ species probed with ethylnitrosourea.

| $tRNA^{Leu}$ species | D-loop[a] (14 to 21) | Levitt pair '15–48' | Variable region[b] (44 to 48) | 23 ; 59 positions | '26–44' pair | '49–65' pair |
|---|---|---|---|---|---|---|
| *Prokaryotic type* (eubacteria and organelles) | | | | | | |
| bean chloroplastic (U*AA) | $\alpha = 4$ ; $\beta = 3$ | A15U48 | L = 16 (l = 3) (bp = 5) | C ; G | Ψ-U | G-C |
| bean chloroplastic (CmAA) | $\alpha = 4$ ; $\beta = 3$ | A15U48 | L = 13 (l = 4) (bp = 3) | C ; G | G-U | G-U |
| bean chloroplastic ($UAm^7G$) | $\alpha = 4$ ; $\beta = 3$ | A15U48 | L = 11 (l = 2 or 4) (bp = 2 or 3) | C ; G | G-U | C-G |
| *Escherichia coli* (CAG) | $\alpha = 4$ ; $\beta = 3$ | A15U48 | L = 15 (l = 4) (bp = 4) | C ; G | G-U | G-C |
| ***Escherichia coli* (GAG)** | $\alpha = 4$ ; $\beta = 3$ | A15U48 | L = 15 (l = 4) (bp = 4) | C ; G | G-U | A-U |
| *Eukaryotic type* | | | | | | |
| **bean cytoplasmic (C*AA)** | $\alpha = 3$ ; $\beta = 4$ | G15$m^5$C48 | L = 15 (l = 4) (bp = 4) | G ; A | Um-A | G-C |
| **yeast cytoplasmic (UAG)** | $\alpha = 3$ ; $\beta = 4$ | G15$m^5$C48 | L = 13 (l = 4) (bp = 3) | G ; A | $m^2_2$G-U | A-U |
| **yeast cytoplasmic ($m^5$CAA)[1]** | $\alpha = 3$ ; $\beta = 4$ | G15$m^5$C48 | L = 13 (l = 3) (bp = 3) | G ; A | $m^2_2$G-U | A-U |

Isoacceptor leucine tRNAs are named according to their anticodon ; those species studied for their interaction with bean cytoplasmic leucyl-tRNA synthetase are written in bold characters. [1]Renaturable species. All leucine tRNAs have an A residue at the discriminator position 73 ; as in other class II tRNAs, the D-stem comprises only 3 Watson-Crick base pairs, the fourth being an anomalous purine13-A22 pair. [a]Length of the two sequences 5′ and 3′ from the two invariant G18G19 residues ; [b]'L' is the length of the variable region and 'l' that of the putative miniloop closing the helical stem in that region ; 'bp' gives the number of putative base pairs in the stem.

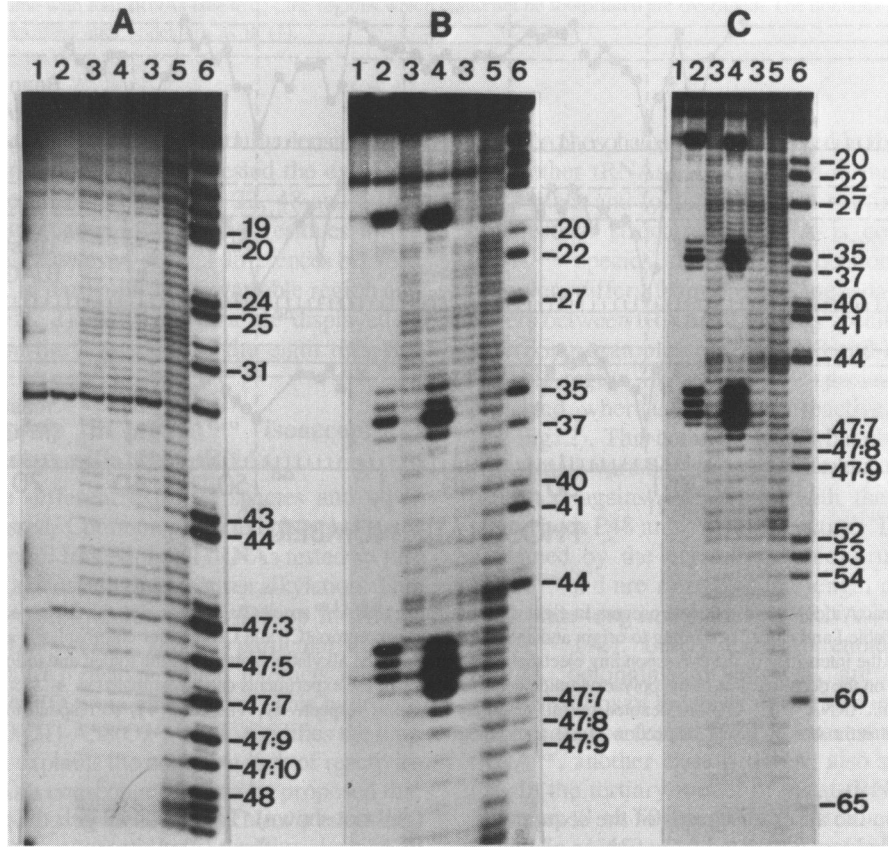


**Fig. 1.** Autoradiograms of 20% polyacrylamide gels showing phosphate alkylation with ethylnitrosourea of 3′ end-labeled bean cytoplasmic $tRNA^{Leu}$(C*AA) (panel A) and *E. coli* $tRNA^{Leu}$(GAG) (panels B and C) either free or interacting with bean cytoplasmic leucyl-tRNA synthetase. Lanes 1 and 2 are control incubations in the absence or presence of leucyl-tRNA synthetase, respectively ; lanes 3 correspond to alkylations of free native tRNA, lanes 4 to alkylations of tRNA in the presence of leucyl-tRNA synthetase and lanes 5 to alkylations of free tRNA under denaturing conditions ; lanes 6 are ribonuclease T1 ladders.

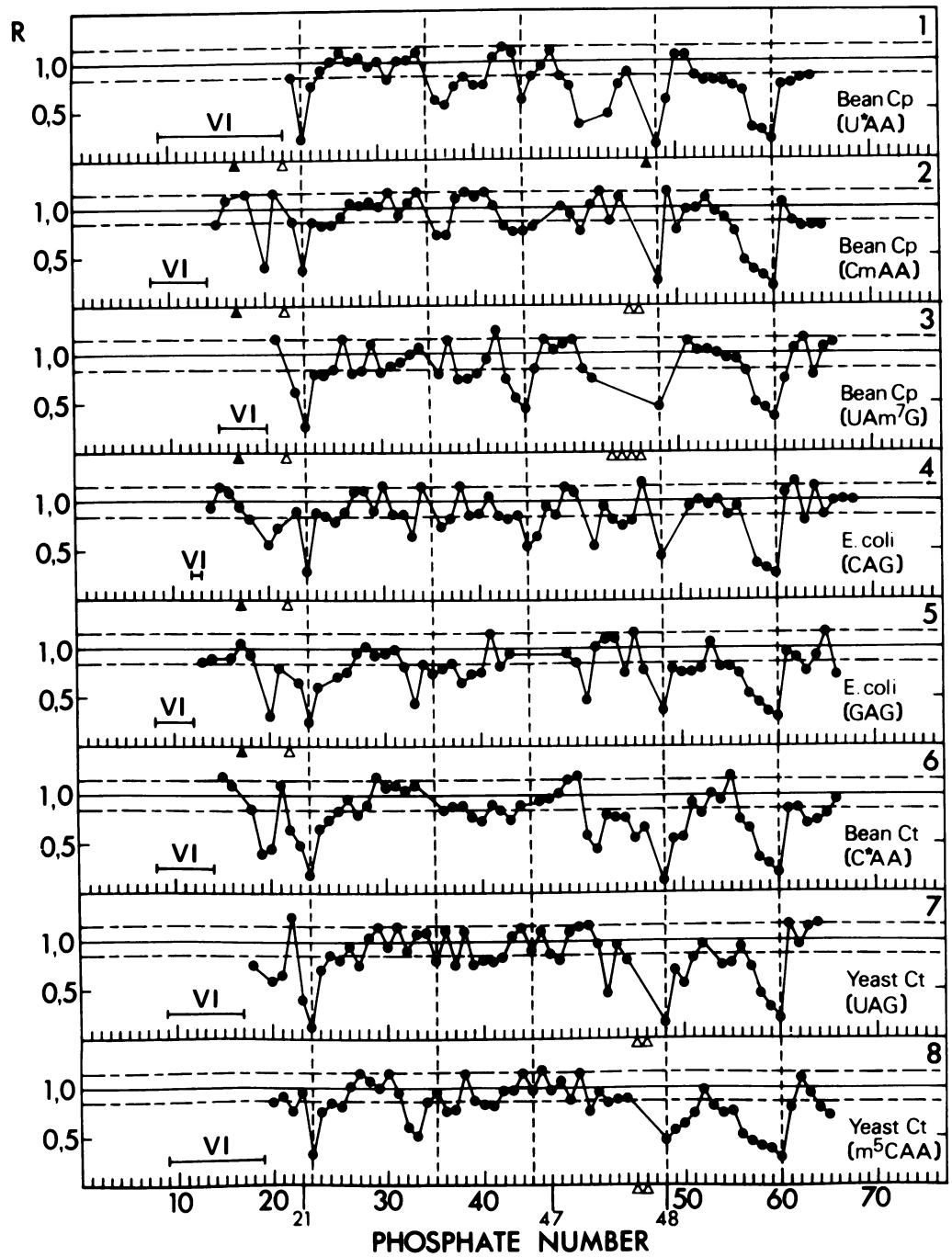


**Fig. 2.** Patterns of phosphate reactivities towards ethylnitrosourea in eight different native $tRNA^{Leu}$ species as compared to the denatured unfolded molecules. Patterns are classified as the tRNAs in Table I and named according to origin and anticodons of isoacceptors (Cp and Ct stand for chlorosplastic and cytoplasmic, respectively). R values are the ratios between the intensities of the corresponding electrophoretic bands in the alkylation patterns of the folded and unfolded tRNAs. These intensities were measured as peak heights on the densitograms of the polyacrylamide gels. Accuracy of the experiments can be estimated as ± 15%. Extra or missing nucleotides by reference to bean cytoplasmic $tRNA^{Leu}$(C*AA) are denoted by full or empty triangles, respectively. The bars (**VI**) correspond to regions in the tRNAs where reactivities of phosphates were estimated by visual inspection of the autoradiograms.

can be readily detected on the autoradiograms of the sequencing gels by comparison with ladders generated from tRNAs alkylated under denaturing conditions. A typical experiment (Fig. 1) gives the alkylation pattern of bean cytoplasmic $tRNA^{Leu}$(C*AA) and *E. coli* $tRNA^{Leu}$(GAG) and clearly shows several protected phosphates (e.g. at positions 22, 48 and 60). Similar mapping experiments were conducted on the six other $tRNA^{Leu}$ species (gels not shown). To note on all gels the presence of several bands in controls without ethylnitrosourea treatment (for instance at position 35 in bean $tRNA^{Leu}$(C*AA)). They are generated by spontaneous hydrolysis, a phenomenon observed with all RNAs tested so far in such experiments (e.g. 29, 30). The occurence of these cuts reflects an intrinsic fragility of the RNAs (for a discussion see 31, 32).

**Table II.** Sequences of the eight $tRNA^{Leu}$ species for their chemical reactivity towards ethylnitrosourea with positions of phosphates protected against alkylation in the native tRNAs (triangles below the sequences) or in contact with bean cytoplasmic leucyl-tRNA synthetase (circles above the sequences).

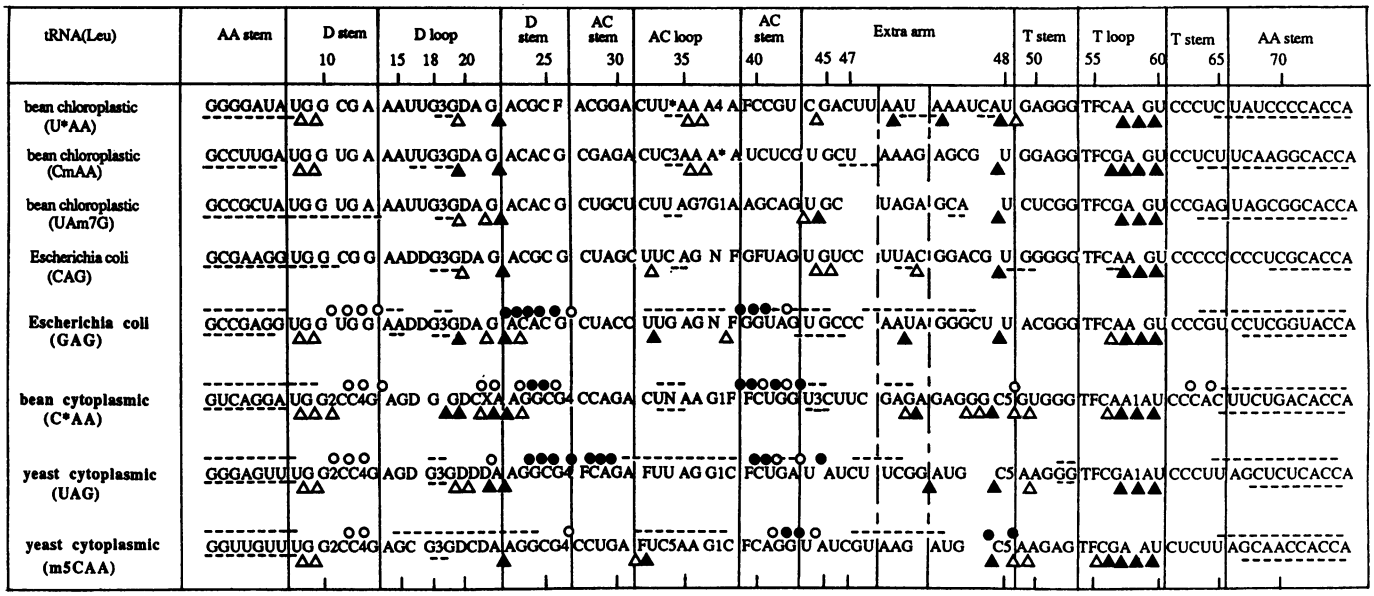


Isoacceptor leucine tRNAs are named according to their anticodon ; those species studied for their interaction with bean leucyl- tRNA synthetase are written in bold character. Full and empty symbols are for strong (R values $\leq 0.5$) and moderate ($0.5 < R \leq 0.7$) protections, respectively ; extremely weak but significant protections ($0.7 < R < 0.85$) are not listed in this compilation. The parts of the sequences which could not be probed in free tRNAs are underlined. Footprinting of the complexes was only done with four tRNAs (see text) ; the regions which could not be footprinted are overlined. The domains in the cloverleaf folding are indicated. Abbreviations for modified nucleotides are as in (1).

A quantitative analysis of the alkylation data by densitometry of the gels clearly confirms for all tRNAs tested the existence of strongly protected phosphates at positions 22, 48 and 60, as well as that of other homologous low reactive residues in the D-loop and T-loop regions. However, several differences between the tRNAs are observed, in particular in the variable region and in the anticodon loop (Fig. 2). All these data are displayed in a comparative fashion on the sequences of the eigth $tRNA^{Leu}$ isoacceptors in Table II.

## Conformational features in $tRNA^{Leu}$ isoacceptors: similarities and differences with other tRNAs

Similarities between the different $tRNA^{Leu}$ species and other tRNAs will first be discussed. Common protected phosphates are mainly located in the T-loop. Indeed, in all tRNAs tested so far, P60 is strongly protected against ethylnitrosourea alkylation. This is linked to the intrinsic conformation of the T-loop in tRNAs first discussed for $tRNA^{Phe}$ (33), and in particular to the presence of the constant C61 residue which interacts through hydrogen bonding with P60(O2) via its N4 atom. This hydrogen bond, together with a P60(O1)-A58(O2′) bond, rigidifies the loop conformation and in turn explains the complete lack of reactivity observed for P60 (15). As a consequence it can be proposed that the conformation of the T-loops in the leucine tRNAs is essentially the same as in other tRNAs. By analogy to what observed in $tRNA^{Phe}$ and $tRNA^{Asp}$ and explained by the crystallographic structures of these tRNAs, the protections of P57 to P59 in T-loops of leucine specific tRNAs most probably are linked to subtle differences in the interactions of these loops with D-loops, leading to steric hindrance phenomena preventing alkylation.

Other phosphates found protected in the leucine tRNAs, as well as in other tRNAs, are clustered in the variable region and in the D-stem and loop. This again confirms that the basic three-dimensional structure of tRNA is conserved in the various $tRNA^{Leu}$ species. The exact location of these phosphates, however, differs from one leucine isoacceptor to another, as it differs between tRNAs of various specificities (e.g. 12, 14, 26). A striking example concerns P48 and P49 at the 3′ end of the variable region. In all $tRNA^{Leu}$ species tested, P48 is strongly protected, whereas P49 is fully reactive or moderately protected (see Fig. 2). This contrasts with what observed in class I tRNAs, with small variable regions, in which P49 is always strongly protected against alkylation, with the exception of $tRNA^{Asp}$ where both P48 and P49 are reactive. These behaviors could be explained by the crystallographic structures of $tRNA^{Asp}$ and $tRNA^{Phe}$ and are related to the length of the variable region, 5 nucleotide-long in most class I tRNAs, and 4 nucleotide-long in $tRNA^{Asp}$ (12). Likely the differential protections in leucine tRNAs, belonging to class II, are linked to the peculiar conformations of the variable regions in these tRNAs (see Table I for sequence features). It is interesting to mention that yeast $tRNA^{Ser}$, another class II tRNA, also shows protections at P48 (7). In the tertiary model of yeast $tRNA^{Ser}$, a sharp turn from residues 48 to 50 has been constructed. Such a conformation would be suitable for a magnesium binding site, thus explaining the non-reactivity of P48 in this tRNA (7). It is tempting to generalize the existence of such a magnesium binding site to $tRNA^{Leu}$ species, which would explain the low reactivity of phosphates at the junction of the variable region and the T-stem.

At the junction of the variable region with the anticodon arm,

P45 is protected in three tRNAs of prokaryotic type out of the 4 species which could be tested for that position ; when testable this phosphate is fully reactive in the eukaryotic species. Adjacent to this position, P46 and P47 are never protected (except for a moderate protection of P46 in *E. coli* $tRNA^{Leu}(CAG)$), in contrast to the homologuous phosphates in yeast $tRNA^{Ser}$ which are partially reactive (7). This suggests a different connection of the variable region to the core of the molecule in the two tRNA families, a possibility also suggested by differential contacts of these two class II tRNAs with their cognate synthetases (see below).

Phosphates protected at variable extents are found in all leucine tRNAs in the 47:1 to 47:11 domain within the large variable region. In most cases these phosphates are located in the putative miniloop (see Fig. 2 and Table II). Protected phosphates within the helices proposed on the basis of sequence information, are only found in two instances at the 3'-side of the variable region of chloroplastic $tRNA^{Leu}(U*AA)$ and bean cytoplasmic $tRNA^{Leu}(C*AA)$. Since phosphates are reactive in regular RNA helices and present protections in loop or higher-order structures (e.g. 12), these data agree with the existence of regular stem structures closed by miniloops in the variable region of leucine specific tRNAs. These stems and miniloops are built up by 3 to 5, and 2 to 4 base pairs and nucleotides, respectively (Table I). The fact that protections in miniloops are not found at homologous positions in all tRNAs, points to the existence of different conformations in these parts, and *a posteriori* of different miniloop lengths. A peculiar tRNA is bean chloroplastic $tRNA^{Leu}(UAm^7G)$ with only 11 nucleotides in the variable region. On the basis of the ethylnitrosourea data it is difficult to prove the existence of a well-ordered stem and miniloop conformation in this tRNA. Note the presence of a stem closed by a three nucleotide miniloop in yeast $tRNA^{Ser}$, as demonstrated by chemical mapping of the bases (7).

The constant protection of P22 is another characteristics of leucine tRNAs. This phosphate, located at the junction of the D-stem and -loop, is also protected in $tRNA^{Ser}$ (7), but not in class I tRNAs (26), except yeast $tRNA^{Asp}$, a tRNA with 4 nucleotides in the variable region (12). In that last tRNA, the protection of P22 is due to hydrogen bonding with A46(N6) in the variable region. In the model of class II $tRNA^{Ser}$, P22 is in close contact with the variable region (7). Likely, such proximity also exists in leucine tRNAs, but the relationship between the region around P22 and the variable region certainly is different in the two families of class II tRNAs. Indeed, whereas P21 is fully protected in $tRNA^{Ser}$, it is only moderately protected or even fully acccessible in leucine specific tRNAs.

All leucine tRNAs exhibit moderate or strong protection at P20, except yeast $tRNA^{Leu}(m^5CAA)$, where this phosphate is fully reactive (see Fig. 2 and Table II). On the contrary, differences

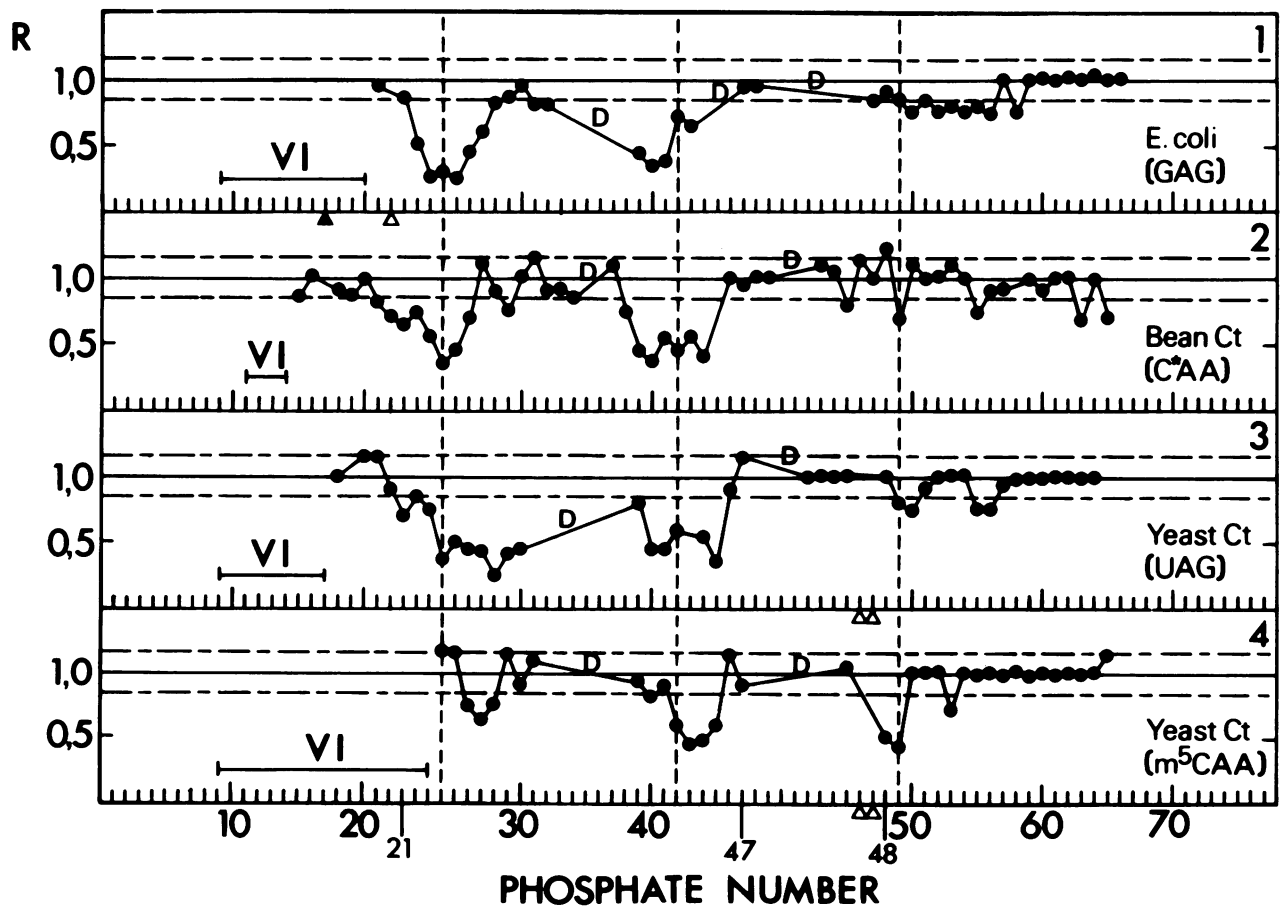


**Fig. 3.** Patterns of phosphate reactivities towards ethylnitrosourea in four different native $tRNA^{Leu}$ species in the presence of bean cytoplasmic leucyl-tRNA synthetase as compared to the free native molecules. Patterns are classified and named as in Fig. 2. R values are the ratios between the intensities of the corresponding electrophoretic bands in the alkylation patterns of enzyme-complexed and free tRNA. The accuracy of the experiments is similar as in Fig. 2. Regions where tRNA degradations induced by leucyl-tRNA synthetase appear are indicated by **D** ; regions where protections were detected by visual inspection of the autoradiograms are indicated by **VI**.

in reactivities are found for P20:1 and P20:2. They could be related with the structural variability in D-loops between leucine tRNAs.

Several protected phosphates, located in the P-10 loop (at positions 9 to 11), were found in all tRNAs which could be tested for this region. In the crystal structure of yeast $tRNA^{Asp}$ and $tRNA^{Phe}$, these phosphates are forming a pocket suitable for a magnesium binding site (e.g. 34, 35). Such a conformation has been introduced in the modelling of yeast $tRNA^{Ser}$ (7) and by similarity can be proposed for $tRNA^{Leu}$.

Non-reactive phosphates are found in the anticodon loop of leucine tRNAs. The protections are mostly weak, but are clearly apparent in five tRNAs, and in two others there is a tendency to lower reactivities (see Fig. 2). In the two *E. coli* tRNAs and in yeast $tRNA^{Leu}(m^5CAA)$, protections occur at position 33, whereas in bean chloroplastic $tRNA^{Leu}(U^*AA)$ and $tRNA^{Leu}(CmAA)$ they occur at P36 and P37. A particular pattern is observed in yeast $tRNA^{Leu}(m^5CAA)$ species (see Fig. 2). Since a magnesium binding site has been found in the anticodon loop of yeast $tRNA^{Phe}$ (36), it is possible that the variations in phosphate reactivities observed in leucine tRNAs reflect different magnesium coordinations and in turn different loop conformations.

In summary, the present phosphate mapping experiments permitted to extract specific structural characteristics in the family of leucine tRNAs, as for example the conformations around P21-22 and P48-49. They showed also striking similarities of leucine tRNAs with tRNAs of other specificities, as for example in the T-loop around P60. In the absence of crystallographic structures, such results give the most precise conformational informations on this family of tRNAs and represent a good starting point for future graphical modelling investigations. Note here studies done in parallel on $tRNA^{Leu}$ from mammalian origin (37), which corroborate some of our conclusions.

## Interaction between $tRNA^{Leu}$ and plant leucyl-tRNA synthetase

In this section, we will describe contact points of four leucine-specific tRNAs with bean cytoplasmic leucyl-tRNA synthetase. This will allow us to define the topology of interaction of these tRNAs with the bean enzyme, but not to define the specificity determinants of $tRNA^{Leu}$, although specificity determinants and contact points can overlap. We note that complementary data obtained on a mammalian leucine-specific tRNA were reported recently (38).

Footprinting experiments were conducted on homologous bean cytoplasmic $tRNA^{Leu}(C^*AA)$, as well as on yeast $tRNA^{Leu}(UAG)$ and $tRNA^{Leu}(m^5CAA)$, complexed to bean cytoplasmic leucyl-tRNA synthetase. It is recalled that the two heterologous yeast tRNAs can be fully charged in the presence of the bean enzyme, which does not aminoacylate isoacceptors from chloroplastic origin (22). Also, *E. coli* $tRNA^{Leu}(GAG)$, which is efficiently charged by this enzyme, was mapped in the presence of bean cytoplasmic leucyl-tRNA synthetase, whereas *E. coli* $tRNA^{Leu}(CAG)$, less efficiently charged ($K_m$ decreased by a factor of ten (22)) was not. This functional difference between the two *E. coli* $tRNA^{Leu}$ isoacceptors for heterologous leucylation might be linked to the nature of their N49-N65 base pair. As proposed earlier, this base pair could be involved in the adaptation of tRNAs to synthetases, and an A49-U65 pair, as in *E. coli* $tRNA^{Leu}(GAG)$ (see Table I), could be more favorable than a G49-C65 pair for heterologous charging (39).

Typical footprints of bean cytoplasmic $tRNA^{Leu}(C^*AA)$ and *E. coli* $tRNA^{Leu}(GAG)$ complexed to leucyl-tRNA synthetase are given in Fig. 1. Interpretation of the gels by densitometry

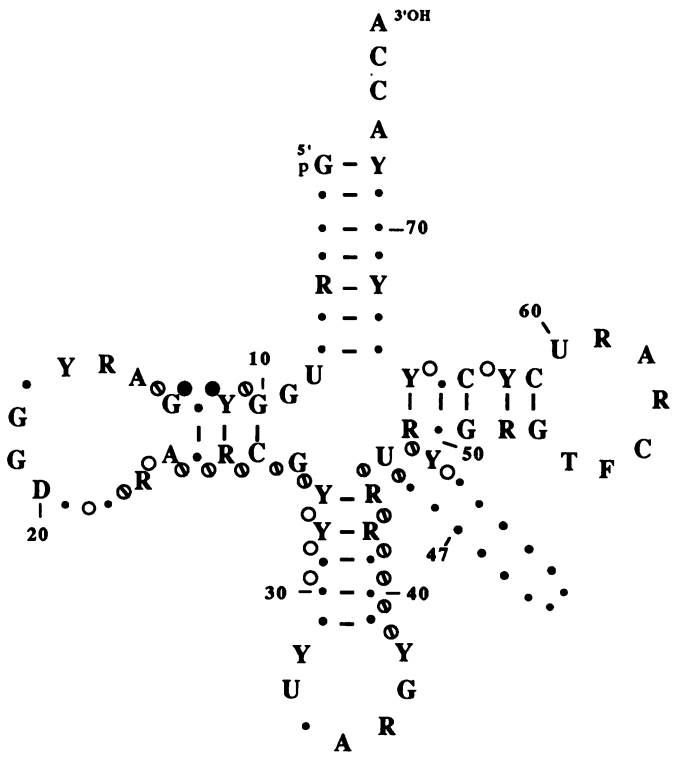


**Fig. 4.** Composite cloverleaf structure of four $tRNA^{Leu}$ species with positions protected by bean cytoplasmic leucyl-tRNA synthetase against alkylation by ethylnitrosourea. The tRNAs studied were the eukaryotic type tRNAs and *E. coli* $tRNA^{Leu}(GAG)$. Only strongest protections, as listed in Table II ($R \leq 0.7$), were taken into account in the comparison. Phosphates protected by leucyl-tRNA synthetase in all tRNAs (●), in at least two of the tested molecules (◑), and in one tRNA (○) are indicated.

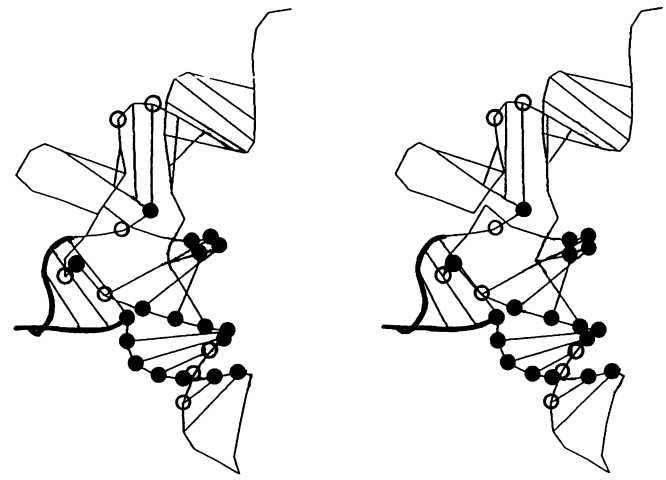

**Fig. 5.** Three-dimensional model of a long variable loop tRNA with phosphates in contact with leucyl-tRNA synthetase. Results are displayed in a phosphate backbone model of $tRNA^{Ser}$ (7), with the variable region in heavy line. Phosphates found strongly protected ($R \leq 0.7$) in all or at least two of the isoacceptor tRNAs tested are indicated by (●) ; those protected by the protein in only one isoacceptor are indicated by (○).

(and when needed by visual inspection) are shown in Fig. 3 and Table II. The synthetic display of all results is given on a composite $tRNA^{Leu}$ sequence in Fig. 4.

Before discussing contact points it is worth mentioning several sites in certain leucine tRNAs sensitive to degradations within the complex with leucyl-tRNA synthetase and which consequently could not be tested for contacts with the enzyme. They are mainly located in the anticodon loop and in the variable region. Similar effects were observed with other tRNAs interacting with synthetases or elongation factor (40), and were interpreted as reflecting conformational changes in tRNA upon protein binding. In the present case, the degradations are almost negligible in the homologous bean cytoplasmic $tRNA^{Leu}$(C*AA), but appear much stronger in the heterologous tRNA species (Fig. 1). Control experiments on yeast $tRNA^{Asp}$ incubated with bean leucyl-tRNA synthetase also revealed cuts in the anticodon loop of this tRNA. These degradations could be avoided in the presence of the RNase inhibitor vanadyl-ribonucleoside complex (from BRL) (41), which could point to the presence of a contaminating RNase activity. However, gel electrophoresis of leucyl-tRNA synthetase did not reveal contaminants and rechromatography of the bean enzyme on agarose-5′-(4-aminophenyl-phosphoryl) uridine 2′(3′) phosphate (from Pharmacia), a specific adsorbent for RNases (42), had no effect on this phenomenon. Therefore it may be suggested that leucyl-tRNA synthetase itself possesses an RNase activity. This view should not be overlooked since it was recently shown that a yeast mitochondrial leucyl-tRNA synthetase is involved in RNA splicing (43). It could be argued that leucyl-tRNA synthetase could generate tRNA fragments of altered conformation which would show new reactivities and thus interfere with interpretation of footprinting data. This latter possibility is unlikely since nicked tRNA does not unfold and consequently should keep its alkylation properties unchanged. Furthermore the extent of these nicks never exceeds 20% of the tRNA molecules so that the extent of putative new reactivities would probably fall within the error range of the method. It could also be argued that optimized footprinting on leucine tRNAs should be conducted in the presence of the vanadyl-ribonucleoside complex. This could not be done since the RNase inhibitor strongly inhibits $tRNA^{Leu}$ charging and modifies the alkylation patterns (e.g. new protections at P54 to P59 in the T-arm and disappearance of those obtained in the absence of the inhibitor), demonstrating *a posteriori* that complexes between leucyl-tRNA synthetase and tRNA are perturbed under those conditions and underlining the correlation between the footprints presented in this work and the existence of specific complexes.

Regions protected by leucyl-tRNA synthetase in all four tRNAs are located at the 5′-side of the D-stem, at the 3′-side of the D-stem including the junction with the anticodon stem, and at the 3′-side of the anticodon stem. Yeast $tRNA^{Leu}(m^5CAA)$, in contrast with the three other isoacceptors, shows weaker although significant protections at the 3′-side of the D-stem, an observation which might be correlated with a less efficient leucylation activity of this tRNA, as reflected by a three times reduced $V_{max}$ compared to that found under similar conditions for the other isoacceptors. Note also the particular alkylation pattern of the P19-P23 region in the free tRNA (Table II), which suggests a particular D-arm conformation in $tRNA^{Leu}(m^5CAA)$ giving raise to looser interactions of this region with bean leucyl-tRNA synthetase. Yeast $tRNA^{Leu}(m^5CAA)$ shows also protections at P48 and P49 (Fig. 3). In bean cytoplasmic $tRNA^{Leu}$(C*AA) and yeast $tRNA^{Leu}$(UAG), P48 could not be tested for interaction with the enzyme, as it is already fully protected in the free tRNAs (Fig. 2). Finally, in the homologous bean tRNA two moderate but significant protections were found at P63 and P65 in the T-stem. Possible contacts at the 3′- and 5′-ends of the tRNAs could not be revealed due to the limits of the footprinting method.

When the set of protection data are confronted to the composite sequence of leucylable tRNAs (Fig. 4) it appears that many contact points overlap with conserved or semi-conserved sequences in the isoacceptors. This is for instance the case for the protected phosphates at the 3′-side of both the D-stem and anticodon stem. As to position 13, found protected in all four tRNAs tested, it corresponds to a conserved G residue. Interestingly, this position 13 is strongly correlated with the function of leucine tRNAs as deduced from a computer analysis of tRNA sequences (9). When all these protection data are displayed on the three-dimensional model of a long-extra loop tRNA (Fig. 5), it appears that protected phosphates lie on both sides of the L-shaped tRNA conformation in such a way that the enzyme would embrace the tRNA by the inside of the L-shape. The variable loop was not found in contact with leucyl-tRNA synthetase.

When compared with other tRNA/synthetase complexes, striking similarities appear with the valine system. Indeed $tRNA^{Val}$ and the tRNA-like structure from turnip yellow mosaic virus present the same geometry of interaction with valyl-tRNA synthetase (16, 44). Note that leucyl- and valyl-tRNA synthetases are monomers of 130,000 daltons with an elongated shape (22, 45). In contrast to leucine and valine specific tRNAs, $tRNA^{Asp}$, $tRNA^{Phe}$, $tRNA^{Thr}$ and $tRNA^{Trp}$ interact with a different geometry with their cognate dimeric or tetrameric aminoacyl-tRNA synthetase (12−14). Thus, the present data on the leucine system agree with the view according to which the structures of synthetases dictate the geometry of interaction of the tRNAs (46). This view implies for other large variable region tRNAs interacting with dimeric synthetases, protein contacts different from those occuring in $tRNA^{Leu}$. This is actually the case for yeast $tRNA^{Ser}$ interacting with dimeric seryl-tRNA synthetase (17). For instance, while no protection of the variable region was observed in the leucine system, specific protections occured in the 46 to 47:2 region of yeast $tRNA^{Ser}$ complexed with seryl-tRNA synthetase.

## ACKNOWLEDGMENTS

We thank M. Arbogast for excellent technical assistance, G. Souciet for collaboration in leucyl-tRNA synthetase preparation, V. Sarantoglou for a gift of an enriched yeast $tRNA^{Leu}$ fraction and A.C. Dock-Bregeon, B. Ehresmann and E. Westhof for help and stimulating discussions. The constant support of J.P. Ebel and J.H. Weil is acknowledged. This work was supported by grants from Centre National de la Recherche Scientifique (CNRS), Ministère de la Recherche et de l'Industrie (MRI), and Université Louis Pasteur (ULP), Strasbourg.

## REFERENCES

1. Sprinzl, M., Hartmann, T., Weber, J., Blank, J. and Zeidler, R. (1989) Nucleic Acids Res., **17**, Supplement r1−r172.
2. Young, D.J., Bock, R.M., Nishimura, S., Ishikura, M., Yamada, Y., RajBhandary, U.L., Labanauskas, M. and Connors, P.G. (1969) Science, **166**, 1527−1532.
3. Spencer, M., Neave, E.J. and Webb, N.L. (1978) J. Chromatogr., **166**, 447−454.

4. Spencer, M., Neidle, S. and Jones, T.A. (1979) Biochem. Biophys. Res. Commun., **86**, 66–70.
5. Dock, A.C., Lorber, B., Moras, D., Pixa, G., Thierry, J.C. and Giegé, R. (1984) Biochimie, **66**, 179–201.
6. Brennan, R. and Sundaralingam, M. (1976) Nucleic Acids Res., **3**, 3225–3251.
7. Dock-Bregeon, A.C., Westhof, E., Giegé, R. and Moras, D. (1989) J. Mol. Biol., **206**, 707–722.
8. McClain, W.M. and Nicholas Jr, H.B. (1987) J. Mol. Biol., **194**, 635–642.
9. Nicholas Jr, H.B. and McClain, W.M. (1987) CABIOS, **3** ,177–181.
10. Watson, J.D., Hopkins, N.H., Roberts, J.W., Steitz, J.A. and Weiner, A.M. (eds) (1987) in 'Molecular Biology of the Gene', fourth edition, vol. 1, chapter 15, Benjamin Cummings Publishing Company.
11. Kisselev, L.L. (1985) Prog. Nucl. Acid Res. Mol. Biol., **32**, 237–266.
12. Romby, P., Moras, D., Bergdoll, M., Dumas, P., Vlassov, V.V., Westhof, E., Ebel, J.P. and Giegé, R. (1985) J. Mol. Biol., **184**, 455–471.
13. Garret, M., Labouesse, B., Litvak, S. Romby, P., Ebel, J.P. and Giegé, R. (1984) Eur. J. Biochem., **138**, 67–75.
14. Théobald, A., Springer, M., Grunberg-Manago, M., Ebel, J.P. and Giegé, R. (1988) Eur. J. Biochem., **175**, 511–524.
15. Romby, P., Carbon, P., Westhof, E., Ehresmann, C., Ebel, J.P., Ehresmann, B. and Giegé, R. (1987) J. Biomol. Struct. Dyn., **5**, 669–687.
16. Vlassov, V.V., Kern, D., Romby, P., Giegé, R. and Ebel, J.P. (1983) Eur. J. Biochem., **132**, 537–544.
17 Dock-Bregeon, A.C., Garcia, A., Giegé, R. and Moras, D. (1990) Eur. J. Biochem., in press.
18. Podjarni, A., Rees, B., Thierry, J.C., Cavarelli, J., Jésior, J.C., Roth, M., Lewit Bentley, A., Kahn, R., Lorber, B., Ebel, J.P., Giegé, R. and Moras, D. (1987) J. Biomol. Struct. Dyn., **5**, 669–687.
19. Pillay, D.T.N., Guillemaut, P. and Weil, J.H. (1984) Nucleic Acids Res., **12**, 2997–3001.
20. Green, G.A., Maréchal, L., Weil, J.H. and Guillemaut, P. (1987) Plant Mol. Biol., **10**, 13–19.
21. Souciet, G., Dietrich, A., Colas, B., Razafimahatratra, P. and Weil, J.H. (1982) J. Biol. Chem., **257**, 9598–9604.
22. Dietrich, A., Souciet, G., Colas, B. and Weil, J.H. (1983) J. Biol. Chem., **258**, 12386–12393.
23. Guillemaut, P. (unpublished result).
24. Osorio-Almeida, M.L., Guillemaut, P., Keith, G., Canaday, J. and Weil, J.H. (1980) Biochem. Biophys. Res. Commun., **92**, 102–108.
25. Rether, B., Bonnet, J. and Ebel, J.P. (1974) Eur. J. Biochem., **50**, 281–288.
26. Vlassov, V.V., Giegé, R. and Ebel, J.P. (1981) Eur. J. Biochem., **119**, 51–59.
27. Kowalski, S., Yamane, T. and Fresco, J.R. (1971) Science, **172**, 385–387.
28. Chang, S.H., Kuo, S., Hawkins, E. and Miller, N.R. (1973) Biochem. Biophys. Res. Commun., **51**, 951–955.
29. Florentz, C., Briand, J.P., Romby, P., Hirth, L., Ebel, J.P. and Giegé, R. (1982) EMBO J., **1**, 269–276.
30. Mougel, M., Eyermann, F., Westhof, E., Romby, P., Expert-Bezançon, A., Ebel, J.P., Ehresmann, C. and Ehresmann, B. (1987) J. Mol. Biol., **198**, 91–107.
31. Moras, D., Dock, A.C., Dumas, P. Westhof, E., Romby, P., Ebel, J.P. and Giegé, R. (1983) in 'Nucleic acids : the vectors of life' (Pullman, B. and Jortner, J., eds) vol. **16**, pp. 403–414, Reidel Publishing Co., Dordrecht.
32. Dock-Bregeon, A.C. and Moras, D. (1987) Cold Spring Harbor Symposia Quant. Biol., **52**, 113–121.
33. Quigley, G.J. and Rich, A. (1976) Science, **194**, 796–800.
34. Quigley, G.J., Teeter, M.M. and Rich, A. (1978) Proc. Natl. Acad. Sci. USA, **75**, 64–68.
35. Westhof, E., Dumas, P. and Moras, D. (1985) J. Mol. Biol., **184**, 119–145.
36. Holbrook, S.R., Susman, J.L., Warrant, W.R., Church, G.M. and Kim, S.H. (1977) Nucleic Acids Res., **4**, 2811–2820.
37. Petrushenko, Z.M., Tukalo, M.A. and Matsuka, G.Kh. (1986) Bioorg. Khimiya, **12**, 1492–1497.
38. Matsuka, G.Kh., Tukalo, M.A. and Petrushenko, Z.M. (1988) in 'Macromolecules in the functioning cell' (Castellani, A., Baldini, C and Volpe, P., eds) pp. 43–48.
39. Guillemaut, P. (1988) Nucleic Acids Res., **16**, 7194.
40. Riehl, N., Giegé, R., Ebel, J.P. and Ehresmann, B. (1983) FEBS Lett., **154**, 42–45.
41. Berger, S.L. and Birkenmeier, C.S. (1979) Biochemistry, **18**, 5143–5149.
42. Wierenga, R.K., Huizinga, J.D., Gaastra, W., Welling, G.W. and Beintema, J.J. (1973) FEBS Lett., **31**, 181–186.
43. Labouesse, M., Herbert, C.J., Dujardin, G. and Slonimsky, P.P. (1987) EMBO J., **6**, 713–721.
44. Florentz, C. and Giegé, R. (1986) J. Mol. Biol., **191**, 117–130.
45. Zaccaï, G., Morin, P., Jacrot, B., Moras, D., Thierry, J.C. and Giegé, R. (1979) J. Mol. Biol., **129**, 483–500.
46. Moras, D., Lorber, R., Romby, P., Ebel, J.P., Giegé, R., Bentley, A.L. and Roth, M. (1983) J. Biomol. Struct. Dyn., **1**, 209–223.